

SSS023-01

Room:IC

Time:May 23 08:30-08:45

The nuclear power plant disaster accompanying a great earthquake and the plan to avoid the disaster

Kozo Takahashi^{1*}

¹None

Nuclear disaster: Luckily or unluckily, we have already experienced nuclear accidents which suggest enough the nuclear disaster.

On March 28, 1979, at nuclear reactor No.2 of Three Mile Island, the core meltdown started six minutes after the fault of the main pump, because the outlet of the backup pump was closed. The evacuation in wide area carried out, because it was feared that both pressure vessel and reactor vessel would explore, and that radioactive dust would fall there, though the radiation was limited as the emergency core cooling system (ECCS) was intermittently operated.

This accident shows that the nuclear disaster may happen, even if the reactor is not operating.

On April 26, 1986, at the reactor No.4 of Chernobyl small nuclear explosion occurred when it started to insert all reactor control rods after the experimental operation at extremely low output power.

This disaster shows that the nuclear explosion may happen when a serious fault occurs or maloperation is carried, during the reactor is operating.

A standard 1Gw nuclear power plant (NPP) of Chubu Electric Power Co. at Hamaoka Japan, for example, when the acceleration of more than 0.15g is sensed, automatically inserts all control rods in 1.5 secs and stops the reaction before a S wave arrives.

Hamaoka plants can resist the shock of up to 2g. But we have experienced more than 2g. In S. Iwate Pref. Eq. (2008/06/13, M: 7.2, Depth: 8km), Tsubakidai St., which is located at the epicentral distance of 19km and at the hypocentral distance of 20.6km, observed the maximum acceleration of 4.1g. The distance between Hamaoka and the top surface of Philippine Sea Plate (PSP), where a great earthquake may occur, measures 15 - 20km. So, it is possible that Hamaoka plants experience more than 2g, and then main pipes are broken, and the loss of cooling water starts, though an ECCS is equipped to avoid the loss, because both probabilities of the break and the failure of ECCS are nearly the same. When cooling water leaks in large quantities, the core meltdown starts in a few minutes, even if the reaction has been stopped then, both pressure vessel and reactor vessel explore, like the reactor of Chernobyl did, and it might happen that the half of our population needs to evacuate, depending on wind direction.

In the case where main pipes are broken and the loss of cooling water starts, during the reactor is operating in full power, both pressure vessel and reactor vessel explore, which will be similar to a uranium bomb, and the magnitude of the disaster will be about 1000 times of that at Chernobyl. This is inferred from that at Chernobyl only one cell of 1661 cells explored.

A plan to avoid the disaster: To avoid these disasters, it is necessary to predict great earthquakes. Before great earthquakes usually extraordinary electric fields have been observed. Before and after S. Suruga Bay Eq. (2009/08/11, M: 6.5, Depth: 23km), anomalous electric pulses were also found. In the case the prediction system that monitor the precursory pulses is established, which can use a lightning location system in common, when a great earthquake of more than magnitude 8 occurs, not only the disaster is prevented by stopping NPP following to the precursor, but also NPP can continue to operate without stopping the plant wastefully for long time when it is clear that the distance to the predicted source region is 100km or more, which is measured as the pulses are located at the accuracy of 10km, and that the magnitude, which is estimated from the quantity of the pulses, is less than 8.

Keywords: nuclear power plant disaster, great earthquake, earthquake directly under the plant

SSS023-02

Room:IC

Time:May 23 08:45-09:00

Transdisciplinary Study on Earthquake-related Diseases (7) For Improving Emergency Ambulance Activities

Yutaka Ohta^{1*}

¹Tono Research Inst of Earthq Science

Under a major title as above we have recently been studying for optimization of ambulance activities at an attack by a significant earthquake. This is just continuous study report. Mizunami city, Gifu prefecture, as a sample area in this study, where our Institute locates, has been operating 3 ambulances and it is in higher level than that of the Japan standards. The activities in ordinary situation are therefore satisfactory as to be able to cover 80 or higher percentage of responses to emergency phone calls by 119. In case when a large earthquake attacks, however, the ambulance activities available get down as low as 10% in immediate stages, and therefore any improvement as either reduction of calls by 119 or quicker turn-around time service of ambulance activity is expected. From this point, we introduced probable strategies via simulation in a previous study. But, no detail examination was introduced to know whether the proposed strategies work well or not. This paper pays special effort for examining the reality of the proposed strategies, obtaining additional field data from the sample area.

What found via the analyses of ambulance activity data are that the ambulance dispatches for lightly suffered patients is still over weighted, and we should recall the primary role of ambulance activities. It is nothing but an activity to assist life saving in emergency situations. In this respect we arrive at a conclusion that no lightly suffered citizens are to be transported in use of a limited number of ambulances, especially in unusual situation as an earthquake attack.

Keywords: Earthquake-related Health Consequences, Seriousness Level, Ambulance Activity, Call-response Rate, Simulation

SSS023-03

Room:IC

Time:May 23 09:00-09:15

Benchmark Tests for Strong Ground Motion Simulations (Part 6: Theoretical Methods, Step 3 & 4)

Yoshiaki Hisada^{1*}, Masayuki NAGANO², Atsushi, NOZU³, Ken MIYAKOSHI⁴, Taro NAKAGAWA⁵, Kimiyuki ASANO⁶

¹Kogakuin University, ²Tokyo University of Science, ³The Port and Airport Research Institute, ⁴Geo-Research Institute, ⁵Fujita Corporation, ⁶Disaster Prevention Research Institute

We have been conducting a series of benchmark tests of the strong motion simulation methods for three years since 2009. We chose the three most popular methods for this purpose: the theoretical methods (the wavenumber integration method, the discrete wavenumber method, and the thin-element method), the stochastic Green function method, and the numerical methods (the finite difference method and the finite element method). In this presentation, we show the results of the theoretical methods for the steps 3 and 4; the former is a point source and the latter is extended sources in flat-layered structures, as shown in the tables 1 and 2.

We have obtained the following conclusions. All the results show good agreements in the assigned frequency range (0 - 5 Hz). However, the results for no-damping media show slight differences at very high frequencies, because some groups used very high-Q values, whereas the other group used the Phinney method. In addition, there are slight differences for the a point source on the free surface and the surface faulting model. This is because that the some use the exact surface source model, and the other used the source slightly under the surface.

Please check the following web site for more details.

<http://kouzou.cc.kogakuin.ac.jp/benchmark/index.htm>

Acknowledgements:

This project is in part supported by a research fund of Ministry of Education, Culture, Sports, Science and Technology of Japan (MEXT), and the Research Center of Urban Disaster Mitigation (UDM) of Kogakuin University.

Table 1 Benchmark tests for the 2010 theoretical methods (Step 3 and 4)

ステップ3 (締切:2010/9/1)			ステップ4 (締切:2010/11/1)				
モデル名	T31	T32	T33	T41	T42	T43	T44
地盤	4層地盤		2層地盤	2層地盤			
液震	あり		なし	あり			
震源	点震源 (深さ 2 km : ガウス型開数)		点震源 (深さ 0 km : ガウス型開数)	横ずれ断層 (上端深さ 2 km : 中村-宮武開数)		横ずれ断層 (上端深さ 0 km : 中村-宮武開数)	
有効振動数	0~5 Hz						
出力点	+002, +006, +010, +030, +050, +100 km (計 6 点)						
				破壊伝播	1km ² 間隔一定	1km ² 間隔ゆらぎ	連続
	0~5 Hz						
	出力点 ±002, ±006, ±010, ±030, ±050, ±100 km (計 12 点)						
				推出波形	1波形	3波形	1波形

Table 2 Material Properties for the four layered model

Layer	Thickness (m)	Vp(m/s)	Vs(m/s)	Density(kg/m ³)	Qp	Qs
1	200	1,800	400	2,000	20f	20f
2	400	2,600	1,000	2,400	30f	30f
3	1,000	4,000	2,000	2,600	40f	40f
4 (Half Space)	∞	6,000	3,464	2,700	70f	70f

注1: Q 値の f は振動数(Hz) 注2: 2層地盤モデルの場合、第3層を厚さ 1 km とする

Keywords: Strong Ground Motion Simulations, Benchmark Test, Theoretical Methods, Wavenumber Integration Method, Discrete Wavenumber Method, Thin Layer Method

SSS023-04

Room:IC

Time:May 23 09:15-09:30

Benchmark Tests for Strong Ground Motion Simulations (Part 7 : Numerical Methods, Step 3 & 4)

Chiaki Yoshimura^{1*}, M. Nagano², S. Aoi³, H. Kawabe⁴, H. Uebayashi⁴, T. Hayakawa⁵, S. O. Citak⁶, Y. Hisada⁷

¹Taisei Co., ²Tokyo Univ. of Science, ³NIED, ⁴Kyoto University, ⁵Shimizu Co., ⁶JAMSTEC, ⁷Kogakuin Univ.

We performed a benchmark test for the strong motion simulation methods using numerical methods (finite differences method and finite element method). Six teams from different institutions solved the same problems with the same subsurface structure models and the same seismic sources. We tested three subsurface models: a four layers model, a torapezoidal sedimentary basin model and a stant basement model. All the results calculated by six teams generally show good agreement to each other. We found minor differences are generated by the difference of property distribution near the irregular layer boundaries.

表 1 2010 年度の数値解析手法の解析条件一覧

モデル名	ステップ3 (締切:2010/9/1)			ステップ4 (締切:2010/11/1)	
	N31	N32	N33	N41	N42
地盤	4層地盤		対称盆地	傾斜基盤盆地	
減衰	あり			あり	
震源	点震源A	点震源B	点震源C	点震源C	点震源D
有効動数	0~2.5Hz			0~2.5Hz	
出力点	21点	19点	21点	21点	21点

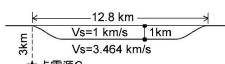
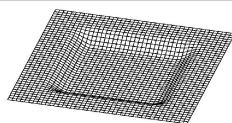


図1 対称盆地 (N33)

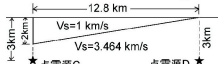
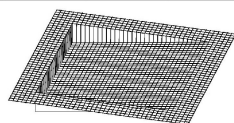


図2 傾斜基盤盆地 (N41, N42)

Keywords: Strong Ground Motion Simulation, Benchmark Test, Numerical Methods, Finite Difference Method, Finite Element Method

SSS023-05

Room:IC

Time:May 23 09:30-09:45

Benchmark Tests for Strong Ground Motion Simulations (Part 8: Stochastic Green's Function Method, Step 3 & 4)

Kenichi Kato^{1*}, Yoshiaki Hisada², Susumu Ohno³, Arihide Nobata⁴, Atsushi Morikawa¹, Yu Yamamoto⁵

¹Kobori Research Complex, ²Kogakuin Univ., ³Tohoku Univ., ⁴Obayashi Co., ⁵Taisei Co.

Since 2009, we performed a benchmark test for the strong motion simulation methods as three years project (Hisada et al., 2011; Yoshimura et al., 2011; Kato et al., 2011). This paper shows the results using stochastic Green's function method.

We have carried out two steps of simple benchmark tests in 2009; one is a point source (step 1) and the other is extended sources (step 2) in homogeneous and two-layered subsurface structures. Radiation coefficient of the source is assumed to be frequency independent, and only SH wave is considered. Site amplification is calculated assuming normal incidence of SH wave. Six groups of researchers/engineers were participated in by using their own methods/codes. Since the simple model is used in the step 1 and 2, all the results calculated by six teams generally show good agreement to each other (Kato et al., 2011).

In step 3 and step 4, more complicated analytical conditions are considered as shown in Table 1. Frequency dependent radiation coefficient of the source is applied, which is the most different conditions in comparisons with step 1 and step 2. Since oblique incidences of both SH and SV waves are considered, vertical component is also generated in addition with horizontal components. All the results of the point source (step 3) and the extended sources (step 4) generally show good agreement to each other in spite of complicated analytical conditions. As for the step 4, we confirmed that the introduction of the random rupture times at the sub-faults are effective to avoid the artificial predominant frequencies caused by the regular intervals of the rupture times. We also found the serious sags in Fourier amplitudes in the middle frequency range around 1 Hz, as compared with the omega-squared model. Since the sags underestimate synthesized amplitude, this problem has to be improved in the future. Synthesized amplitude shows variation in particular frequencies, because random numbers are used in generating time histories and so on. When applying the stochastic Green's function method, this variation should be in mind. Please check the following web site for more details.

<http://kouzou.cc.kogakuin.ac.jp/test/home.htm>

Acknowledgments:

This project is in part supported by a research fund of Ministry of Education, Culture, Sports, Science and Technology of Japan (MIEXT), the Research Subcommittees on the Earthquake Ground Motion of the Architectural Institute of Japan, and the Research Center of Urban Disaster Mitigation (UDM) of Kogakuin University.

References:

Hisada et al., benchmark tests for strong ground motion prediction methods -Case for theoretical methods (Part 1)-, AIJ J. Technol. Des. Vol. 17, No.35, 43-48, 2011.

Kato et al., benchmark tests for strong ground motion prediction methods: Case for stochastic green's function method (Part 1), AIJ J. Technol. Des. Vol. 17, No.35, 49-54, 2011.

Yoshimura et al., benchmark tests for strong ground motion prediction methods: Case for numerical methods (Part 1), AIJ J. Technol. Des. Vol. 17, No.35, 67-72, 2011.

Table 1 Benchmark tests for stochastic green's function method in 2010

モデル名	ステップ3 (点震源)				ステップ4 (面震源)			
	S31	S32	S33	S34	S41	S42	S43	S44*
地盤	一様地盤	2層地盤		4層地盤	2層地盤			
入射角	鉛直	斜め入射			斜め入射			
Q値	なし	あり			あり			
震源	点震源				横ずれ断層	逆断層	横ずれ断層	
干渉イオン (SH & SV)	振動数 (f) 一定		振動数 (f) 依存		振動数 (f) 依存			任意
破壊開始時間					一定	ランダム	一定	
有効振動数	0~20 Hz				0~20 Hz			
出力点	000, +002, +006, +010 (計4点)				000, ±002, ±006, ±010 (計7点)			
出力成分	水平2成分	水平・上下3成分			水平・上下3成分			
乱数の設定	各自の乱数3パターン				各自の乱数3パターン			

注*) S44はオプションケースで自由参加。近地項や中間項の考慮など各自のオリジナル手法を考慮

Keywords: Strong motion prediction methods, Benchmark tests, Stochastic Green's function method, Random numbers, Point source, Fault model

SSS023-06

Room:IC

Time:May 23 09:45-10:00

Ground motion duration and earthquake magnitude

Tetsu Masuda^{1*}

¹ERI, University of Tokyo

Stochastic Green's function method is one of the useful tools to calculate ground motions. To account for the effects of asperities and rupture propagation, the entire fault of dimension L is sub-divided into small sub-faults of dimension R , and ground motions from all sub-faults are integrated instead of evaluating from a point source. Though the size of element is arbitrary, the final synthesized ground motion must not depend on the sub-fault size. Stochastic Green's function is based on the product of Gaussian time series and envelope shape function $e(t)$. In many cases, duration T_r of the envelope shape function is set as inversely proportional to the corner frequency f_c of sub-fault, or in other words, as proportional to the dimension of sub-fault R .

$$T_r = d/f_c = (d/C_c)(R/V_s) \dots (1)$$

When a point source is assumed, total duration of ground motion T is coincide with the envelope function duration,

$$T = T_r = (d/C_c)(L/V_s) \dots (2)$$

The total duration of synthesized ground motion T is the sum of time for the rupture T_p to propagate the entire fault and the duration of sub-fault ground motion T_r .

$$T_p = C_p(L/V_s) \dots (3)$$

$$T = T_p + T_r \dots (4)$$

Generally, equation (2) for a point source and equation (4) for finite source give different values of ground motion duration. As the sub-fault size gets small, the sum also gets small, and the synthesized ground motion does depend on the sub-fault size. Ground motion duration is dependent not only on terms related to the seismic source, such as rupture propagation time T_p and sub-fault duration T_r , but also on terms T_m attributed to the medium, such as reflections and scattering. Therefore, the ground motion duration is expressed as,

$$T = T_m + T_p + T_r \dots (5)$$

As the entire fault size L increases as the earthquake magnitude increases, the total duration of ground motion also increases as the magnitude increases. Equation (5) gives a different relationship between ground motion duration and magnitude from equation (2).

In order to clarify which is more acceptable, I investigated the dependency of ground motion duration on earthquake magnitude. I analyzed big earthquakes and their aftershocks which recently occurred in and around Japan. They include shallow crustal earthquakes, inter-plate earthquakes, and intra-plate earthquakes. The magnitude ranges from 3.6 to 8.0. The observed records from K-NET and KiK-net of NIED and JMA are used. There is variety of definition of ground motion duration. In this paper, I adopted the T_w defined in Boore's envelope shape function, accounting for stochastic Green's function method for strong ground motion prediction.

$$e(t) = a t^b \exp(-ct), t > T_s \dots (6)$$

$$T_w = b/c/0.2 \dots (7)$$

where t is time, the parameters a , b , and c determines the envelope shape, T_s is the arrival time of S wave. Equation (6) is fit to the envelope of observed records of each observation and from each earthquake, the unknown parameters a , b , c , and T_s being determined by the least squares method. The duration of ground motion is calculated by using equation (7).

The following results are obtained.

1. Ground motion duration strongly depends on epicentral distance.
2. Ground motion duration depends on earthquake magnitude.
3. Ground motion duration also depends on velocity structure near the observation station. Longer duration is observed for longer characteristic period of ground.
4. For earthquakes with small magnitude, ground motion duration is not so short as expected from equation (4).
5. Equation (5) better explains the observed ground motion duration.

Keywords: ground motion duration, earthquake magnitude, rupture propagation, rise time, strong ground motion prediction, stochastic Green's function

SSS023-07

Room:IC

Time:May 23 10:00-10:15

Multi-GPU-accelerated simulation of seismic wave propagation for models with land-ocean topography

Taro Okamoto^{1*}, Hiroshi Takenaka², Takeshi Nakamura³, Takayuki Aoki¹

¹Tokyo Institute of Technology, ²Kyushu University, ³JAMSTEC

Accurate simulations of seismic wave propagation using the heterogeneous Earth model is essential in evaluating the strong ground motions due to earthquakes. Recent study with realistic models of land topography and oceanic layer have been revealing their effects on the seismic ground motions (e.g., Nakamura et al., AGU Fall Meeting, 2009). Thus the effects of the land-ocean topography need be incorporated in the simulations and be studied further for better understanding of the ground motions. In order to include those effects, we have recently proposed a unified approach (Takenaka, SEGJ 2009) to model structures with both the irregular free-surface (i.e., land topography) and the irregular water-solid interface (e.g., ocean bottom) in 3D seismic modeling with the finite-difference method (FDM). The approach allows to incorporate the effect of land-ocean topography with sufficient accuracy.

Thus, we implement the unified approach into multi-GPU finite-difference method (FDM) program. The GPUs are adopted to accelerate the simulations because, not only the accuracy, but also the efficiency (performance) of the numerical method is important for the simulation of the seismic wave propagation. GPU (Graphics Processing Unit) is a remarkable device for its many core architecture and for its high memory bandwidth. Recent GPU delivers extremely high computing performance (more than one TFlops in single-precision arithmetic) at a reduced power and cost compared to conventional CPUs.

In this talk we present examples of the simulations by using the new TSUBAME-2.0 grid cluster in the Global Scientific Information and Computing Center, Tokyo Institute of Technology. TSUBAME-2.0 is equipped with 4,224 NVIDIA M2050 GPUs and is ranked as world fourth fastest supercomputer in the recent TOP-500 list. Our MPI-parallel FDM program with the three-dimensional domain decomposition have achieved a performance of about 42.7 TFlops by using 1,200 GPUs so far. The weak scaling was nearly proportional to the number of the GPUs. We will also present some examples of visualization of the wave propagation for realistic land-ocean model.

Keywords: GPU, seismic wave propagation, finite-difference method, topography, ocean bottom topography

SSS023-08

Room:IC

Time:May 23 10:15-10:30

Low-frequency seismic wave simulation with tuned 1-D structure

Tatsuhiko Saito^{1*}, Youichi Asano¹, Yoshihiro Ito², Katsuhiko Shiomi¹

¹NIED, ²Tohoku University

High-quality seismograms recorded by nation-wide seismic network, Hi-net, provide a good opportunity for examining our understanding of earthquake related phenomena, or the performance of the quantitative modeling. The purpose of this study is to examine the performance of 1-D velocity structure models for simulating low-frequency (0.02 - 0.05 Hz) seismic wavefield. We investigated the performance of the conventional 1-D velocity structure model which is used for the estimation of CMT solution in Japan, and a new 1-D velocity model we proposed in this study.

First, we proposed a new 1-D velocity model based on the dispersion relations for Rayleigh and Love waves. The dispersion relations were obtained by the array analysis of Hi-net records of huge teleseismic events ($M > 8.0$). Although the conventional model fails to reproduce the observed dispersion relations, a new model which is characterized by 4 % decrease in S-wave velocities in crust and 2 % decrease in mantle can reproduce the observed dispersion relation well in the frequency range of 0.01 Hz - 0.1 Hz for both Rayleigh and Love waves.

Then, we confirmed the superiority of the new model in the point of the performance of simulating low-frequency (0.02 - 0.05 Hz) seismic-wave propagation over Japan from large earthquakes ($6.0 < M < 6.8$). We confirmed that the new velocity model was able to simulate the observed seismograms better than the conventional velocity model for many earthquakes. The new model, in particular, can simulate better the travel times of surface waves for long epicentral distance ($> \sim 400$ km). Furthermore, the centroid times obtained by the new model are systematically (~ 2 sec) earlier than those by the conventional model.

Through this study, we proposed a new 1-D velocity model, which have better performance for simulating low-frequency seismic waves than the conventional model. The performance of the simulation is significantly improved for many cases but not for all the earthquakes we analyzed. For example, when the surface waves passing through Hida Mountains, the central part of Japan, we cannot well simulate the seismograms. To overcome this limitation, it would be important to extend the velocity model to have spatial varying Moho.

Keywords: Seismic wave, Simulation

SSS023-09

Room:IC

Time:May 23 10:45-11:00

Spectral Amplification Factors for Long-Period (3 to 10 s) Ground Motions in and around the Los Angeles Basin during the

Ken Hatayama^{1*}, Erol Kalkan²

¹Nat'l Res. Inst. of Fire and Disaster, ²U.S. Geological Survey

Mw7.2 El Mayor-Cucapah earthquake that occurred near the U.S.-Mexico border on April 4, 2010 is the first event providing a number of high-quality recordings to study long-period (3 to 10 s) ground motion amplification in and around the Los Angeles (LA) basin. In the LA basin, about 300 km away from the source, higher PGV values (~ 0.1 m/s) of long-period ground motions were observed relative to its surrounding area. By using more than 200 records from this event, spectral amplification factors of long-period ground motions were evaluated in and around the LA basin with respect to reference hard-rock sites. The main observations of this evaluation are the following: (1) Relative to the hard-rock reference sites, the maximum amplification is about a factor of 5 at 8 and 10 s periods in the central part of the LA basin, where depths of V_s 3.2 km/s and V_s 2.8 km/s isosurface according to the latest Southern California Earthquake Center Community Velocity Model (SCEC CVM-H 6.2) are correlated strongly with the observed high amplification; (2) in the San Gabriel valley, located northeast of the LA basin, the maximum amplification is about a factor of 3 at 8 s, and it is correlated well with the depth of V_s 1.5 km/s isosurface; (3) the largest amplification reached to a factor of 10 at the 6 s in the western part of the LA basin (Manhattan Beach), where the SCEC CVM-H 6.2 failed to provide the feature of the underground structures corresponding to the observed high amplification. The observations (1) and (2) mean that there is no single V_s isosurface that represents spatial variations of the long-period ground motion amplification observed in and around the LA basin. Finally, we compared the spectral amplification factors from the observations with those from the simulations using a simple point-source model and the SCEC CVM-H 6.2. Although the simulation results generally agree with the observations for spatial variation of amplification factors at long periods over 8 s, they tend to overestimate the intensity of amplification factors. Including Q-values and/or using detailed source model might improve the agreement between simulations and observations.

Keywords: long-period ground motions, Los Angeles basin, El Mayor-Cucapah earthquake, spectral amplification factors

SSS023-10

Room:IC

Time:May 23 11:00-11:15

3-D underground structure model and simulation of seismic motions in the Mikawa area, Aichi prefecture

Koichiro Saguchi^{1*}, Kazuaki Masaki²

¹Nihon Emsco Ltd., Co., ²Aichi Institute of Technology

Mikawa area is one of the most eminent industry one in Japan and when Tokai and Tonankai earthquake will occur in the near future, it concerned that large economic and human loss will happen in this area. However, three dimensional under ground structural model is not clear still enough for the estimation of the strong ground motions in this area. In this study, we constructed the seismic observation net (Ai-net) in the Mikawa area and we estimated the three dimensional under ground structural model using the receiver function method from the obtained records at Ai-net To accomplish it, we simulated seismic ground motions at observation sites at the Ai-net using the three-dimensional finite element method

The seismic ground motion array observation has been continued after 2005 in the Miakwa area. Acceleration type strong motion seismometers with three components were installed at 30 sites in this area. We calculated the receiver functions from 7 seismic records obtained at each station, and we identified the underground structural model using the simulated annealing method (Ingber (1989)). Based on numerical experiments it is indicated that P-wave velocities, S-wave velocities and Q values of individual layers are inverted very well. Moreover, we constructed the three dimensional under ground structural model in this area obtained from P-wave and S-wave velocity profiles of thick sediments at each station.

Finally, we simulated seismic ground motions at observation sites at the Ai-net using the three-dimensional finite element method considering three-dimensional velocity structure down to 10km. The results indicate that the maximum accelerations in simulated waveforms were similar to the observed one.

Keywords: 3-D underground structural model, simulation of the seismic ground motion, finite element method, seismic observation

SSS023-11

Room:IC

Time:May 23 11:15-11:30

Estimation of Rayleigh wave group velocity in the 1891 Nobi earthquake fault system using seismic interferometry

Hiroaki Sato^{1*}, Masayuki Kuriyama¹, Yasuhira Aoyagi¹, Yoshiaki Shiba¹, Sadanori Higashi¹

¹CRIEPI

During the 1891 Nobi earthquake, it was well known that the successive rupture of some major active faults have occurred about 80 km long in the NE-SW direction. In order to investigate a triggering mechanism of successive rupture of several active faults, it is important to estimate seismic velocity structure in the fault area of this earthquake. In the previous study we have used seismic tomography to estimate velocity structure in the northern part of the 1891 Nobi earthquake fault area by the microearthquake observation. In this research we tried to estimate Rayleigh wave group velocity in the above area using seismic interferometry by a long-term continuous measurement of microtremors.

The three-month continuous measurements of microtremors are conducted at 19 sites in and around the 1891 Nobi earthquake fault system with a receiver spacing of from about 10 to 20 km. The data were processed with seismic interferometric procedure to retrieve Green's function between receivers. We are successful to extract Green's function from stacking of cross-correlation between the two measurements sites using over 30 days of data. The dispersive characteristics of Rayleigh wave were found in the vertical component of observed Green's function of the period range from 0.5 to 8 sec using multiple filter technique. The group velocities of Rayleigh wave in the northern part of the 1891 Nobi earthquake fault area were estimated from the group delay time of two station pairs. As a result, the group velocity between the receivers in the northwestern part of this area (along the Nukumi fault) is high in the period range from 1 to 3 sec and the same in the period range over 3 sec compared to the one in the southwestern part (along the Neodani and Ibigawa fault). In the station pairs across the step between the Nukumi and Neodani fault, the low group velocity is derived in the period range from 3 to 6 sec. These results are able to be well explained by the previous results from seismic tomography.

Keywords: the 1891 Nobi earthquake, Seismic interferometry, Microtremor, Group velocity, Active fault

SSS023-12

Room:IC

Time:May 23 11:30-11:45

H/V spectral ratio of microtremors and velocity structure in the Mexico basin

Shinichi Matsushima^{1*}, Takanori Hirokawa², Yuhei Nitta², Fumiaki Nagashima², Francisco J. Sanchez-Sesma³, Hiroshi Kawase¹

¹DPRI, Kyoto University, ²Grad. School Eng., Kyoto University, ³Instituto de Ingenieria, UNAM

It is essential to detect the subsurface velocity structure beneath urban area to mitigate seismic disaster. In order to estimate the velocity structure, we have proposed a new theory to calculate the H/V spectral ratio assuming that wave propagation is completely diffuse. We measured microtremors in five sites in the Mexico basin, where there were severe damage during the 1985 Michoacan Earthquake several hundreds of kilometers away from the source region, to obtain data so that we can compare the observed H/V spectral ratios to the theoretical ones to check if our theory is applicable. Among the three stations observed in downtown Mexico City which are in a 1km range from east to west, at the most western site Plaza Cibeles, the H/V spectral ratio of NS and EW components look alike and has a peak of about 0.6Hz. The middle site Plaza Rio de Janeiro has a peak of about 0.5Hz for both NS and EW components. Jardin Pushkin, the most eastern site has two peaks for NS component, 0.5 and 0.7Hz respectively, and for EW component the peak is at 0.6Hz. Previous studies show that the predominant frequency for H/V spectral ratio of strong motions at Plaza Ciberes is about 0.5Hz (Salinas, 2010). On the other hand, the peak at Coyoacan, which is in the south part of Mexico City, is around 1.4Hz for NS and EW components and at CENAPRED, which is sitting on lava outcrop has no apparent peak. We will make detail analysis of the data and compare with the theoretical H/V spectral ratio calculated by our new theory from previously known velocity structures.

Keywords: Mexico Basin, Microtremor, H/V Spectral Ratio, Diffuse Field, Velocity Structure

SSS023-13

Room:IC

Time:May 23 11:45-12:00

Site amplification factors derived from coda normalization method (4) amplification factors at borehole and surface

Teito Takemoto^{1*}, Takashi Furumura², Takuto Maeda², Shinako Noguchi²

¹ERI, the Univ. of Tokyo, ²CIDIR, the Univ. of Tokyo

Introduction

We have estimated broad band ($f = 0.5$ -1, 1-2, 2-4 and 4-8 Hz) site amplification factor at each site of the KiK-net and F-net strong motion network in Japan based on the coda normalization method. Estimated amplifications are applied for shaking intensity to show the validity of our estimates on the site amplification factors at each site and in frequencies (Takemoto *et al.*, 2009). Comparison between free surface and borehole in Northeastern Japan revealed that site amplification factors dramatically differ over 2 Hz (Takemoto *et al.*, 2010).

In this study, we used simultaneous inversion of KiK-net borehole and surface stations and F-net stations in whole of Japan to discuss S-wave amplification characteristic at borehole and surface stations in quantitative form.

Data and Method

We used KiK-net surface and borehole stations and F-net nation-wide strong motion network developed across Japanese Islands. Using waveform data of acceleration record from 48 moderate earthquakes, we estimated the site amplification characteristic at each station in four frequency bands ($f = 0.5$ -1 Hz, 1-2 Hz, 2-4 Hz, and 4-8 Hz).

The distribution of the site amplification characteristic in each frequency bands has been estimated by inversion. We assumed an F-net broadband seismic observation station installed in the basement rock site as unity (0 dB) site amplification.

Results

In the high-frequency band ($f = 4$ -8 Hz), absolute value of the site amplification factor in the borehole is smaller than that of the on free surface. Site amplifications in borehole concentrate around 0 dB. The spatial distribution pattern of the site amplification factor is poor correlated between free surface and in the borehole (correlation coefficient $r = 0.52$). High-frequency wave has short wavelength and affected by small scale (< 100 -200 m) structure.

On the other hand, there is little difference between spatial distribution of site amplification factor at borehole and surface stations ($r = 0.88$) in low frequency band ($f = 0.5$ -1 Hz). A few stations showed very high amplification (> 20 dB) in both surface and borehole. Some stations showed small amplification around 0 Hz. Site amplifications in low frequency band have large deviation.

Acknowledgement

We acknowledge the National Research Institute for Earth Science and Disaster Prevention, Japan (NIED) for providing the KiK-net and F-net waveform.

Keywords: coda normalization, site amplification

SSS023-14

Room:IC

Time:May 23 12:00-12:15

Spatial interpolation of empirical amplification factors for response spectra of long-period ground motions

Toshimi Satoh^{1*}, Izuru OKAWA¹, Takao NISHIKAWA³, Toshiaki SATO⁴

¹Ohsaki Research Institute, ²Building Research Institute), ³Tokyo Metropolitan University, ⁴Shimizu Corporation

We (Satoh et al, 2010) developed attenuation relations of acceleration response spectra with a damping factor of 5 % in a period range from 0.1 to 10 seconds including long period using many strong motion records observed at about 1870 stations to make design spectra for long-period structures. In the attenuation relations, amplification factor at each station was obtained, and so the long-period ground motions can be predicted at the stations considering the site-specific amplification factors. In this study we develop empirical regression relations to spatially interpolate the amplification factors in order to predict long-period ground motions at any places in the Kanto basin, the Nobi basin, and the Osaka basin. In addition we put a theoretical interpretation on the empirical relations.

In previous attenuation relations for long-period ground motions, the depth of the seismic bedrock with S-wave velocity of around 3.0 km/s, the depth of the hard rock overlaid on the seismic bedrock, or the combination of one of them and Vs30 (the average S-wave velocity down to 30 meters) are used as parameters for the empirical relations of amplification factors. The reason why the depths were used is that the depth information is easier to obtain than the velocity structure information. In 2009, long-period ground motion maps and the three-dimensional velocity structure models were open in public by the Headquarters for Earthquake Research Promotion in ministry of education, culture, sports, science and technology, Japan. In this study we calculate the average propagation time Tz3.2 from the seismic bedrock with the S-wave velocity of 3.2 km/s to the engineering bedrock using the velocity structure models and develop empirical regression relations of amplification factors using Tz3.2.

It is found that the logarithm of the empirical amplification factors C are represented bi-linear-type regression lines with the connection Tz3.2 of 1 second in a period range from 0.5 to 10 seconds in three basins. The C is modeled by the equations (1) and (2).

$$\log_{10}C = a_1 + b_1 Tz_{3.2} \quad (Tz_{3.2} > 1.0) \quad (1)$$

$$\log_{10}C = a_2 + b_2 Tz_{3.2} \quad (Tz_{3.2} < 1.0) \quad (2)$$

Here a₁, a₂, b₁, and b₂ are regression coefficients. The correlation between C and Tz_{3.2} is better than that between C and the depth of the seismic bedrock. We simulate the C at eight stations in three basins using the regression relations and confirm that the regression relations reasonably represent the C by considering the standard deviations of the regression relations and the standard deviations of C.

Then we put a theoretical interpretation on the empirical relations of the amplification factors using medium responses. First, we calculate medium responses of the fundamental mode of the Love waves and Rayleigh waves from the velocity structures just beneath the observation stations using the three-dimensional structure models. Secondly, we get horizontal components of the Rayleigh waves multiplying the medium responses by horizontal-to-vertical spectral ratios of the Rayleigh waves. Then we add the medium responses of Love waves to them and define them as MR in this study. Finally we analyze the relation between MR and C at each period. It is found that the relation between Tz_{3.2} and logarithm of MR is correlated well with the relation is between Tz_{3.2} and logarithm of C. This results suggest that the empirical regression relations of the equations (1) and (2) have the theoretical basis.

Acknowledgements: The authors express their sincere thanks to the members of the Committee on the Study of the Long-Period Strong Motions and the Working Group on Strong Motions and Responses for their relevant ideas and suggestions. The financial support of the Japan Ministry of Land, Infrastructure, Transport and Tourism is also acknowledged.

Keywords: long-period ground motions, empirical attenuation relations, amplification factors, velocity structure model, medium response

SSS023-15

Room:IC

Time:May 23 12:15-12:30

Evaluation of Site Effects for Acceleration Response Spectra based on Recorded Data

H. Serdar Kuyuk^{1*}, Hongjun Si¹, Kazuki Koketsu¹, Hiroe Miyake¹

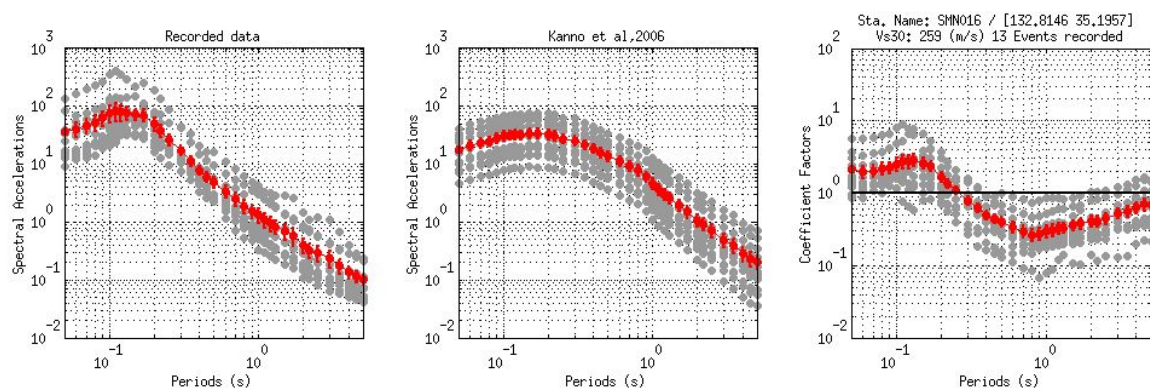
¹Earthq. Res. Inst., Univ. Tokyo

Figure 1. a) Attenuation model for acceleration response spectra proposed by Kanno et al. b) acceleration response spectra using observed records c) site effect correction factors

Seismic networks, such as KIK-net and Hi-net, provide valuable information for studies in engineering and seismology. Research related to the site effect of strong ground motion attenuation use the soil information (especially those extracted from V_{s30}) of the stations. Many other studies have been concerned with V_{s30} at K-NET stations assuming this is the parameter that correlates with site effect. On the other hand, some networks (more than 1000 locations) that are operated by JMA or local prefectural administrations do not have soil information. While V_{s30} is debated as the correct factor to evaluate site effects, Si et al, (2010) have proposed an effective yet easy methodology to assess site effect in attenuation relationships. This correction factor (CF) for site effect is not a function of V_{s30} but instead is dependent on previous recordings. It is calculated by employing an average operator of the ratio of observed ground motion to a reference attenuation model. The advantage of the method is that the site effect can be estimate without soil information.

Kanno et al, (2006) proposed a standard attenuation relation considering acceleration response spectra for Japan. They used a CF function of V_{s30} which were determined from KIK-net stations and summed these with spectral amplitudes in particular frequencies. They applied the CF to their data and were able to reduce the standard error. We use this attenuation relationship as a reference model in our analysis. The method was tested in an area bounded by 133-135E longitude to 32-36N latitude in which 152 K-NET stations are located. We focus on the Tottori region and have evaluated 46 crustal earthquakes with $M_w > 4.0$. From over 7000 records we extracted 596 records that satisfied two criteria a) the stations were within 100 km hypocentral distance and b) the recorded seismic signal was larger than 10 gal.

The acceleration response spectra calculated attenuation model by Kanno et al, (2006) is shown in Figure 1a. Here, the K-NET station SMN016 with a V_{s30} value of 259 m/s is given as an example. Figure 1b is acceleration response spectra estimated from 13 events recorded at that station from 1997 to 2010. The coefficient factors are plotted in Figure 1c. We observed that the method gave sufficiently good results if there are adequate station records. We find good agreement between our results and previously methods that use V_{s30} . Thus, the methodology used in this study is an alternative method for evaluating site effects to obtain more reliable attenuation relationship models.



Keywords: Site effects, acceleration response spectra, Tottori region

An attempt to replicate the so called "trampoline effect" in computational geomechanics

Akira Asaoka^{1*}, Toshihiro Noda², Shotaro Yamada², Takaine Toshihiro³

¹Association for the Development of Earth, ²Nagoya University, ³Asanuma co., ltd.

A loosely deposited alluvial sand subjected to a small seismic motion will initially pack together more firmly. But when a large shearing force is repeatedly brought to act on this well compacted soil, the sand will loosen up again and gradually start to swell. In the first stage of the research reported here, the SYS Cam-clay model proposed by the authors¹⁾ to represent the soil skeleton's elastoplastic constitutive equation is used to replicate a soil behavior of this kind. This model of the elastoplastic constitutive equation is arrived at by incorporating the evolution behaviors of three constituent conceptual of the soil skeleton (structure, overconsolidation, and anisotropy) into the Cam-clay model; the combined model is then capable of reproducing the mechanical behaviors of all soil types from sand to clay, including any intermediate types.

Keeping this representation of the soil skeleton behavior in mind, the present research goes beyond it in using the soil-water coupled finite deformation analysis code **GEOASIA**²⁾, created by mounting the SYS Cam-clay model onto the constitutive equation, to show what occurs when a ground in an overconsolidated state is subjected to an additional strong seismic motion; the soil becomes progressively looser, which may lead to swelling and rising in the ground. The **GEOASIA** analysis code makes it possible to carry out a time history analysis of the phenomena taking place in the ground and in the soil structures resting on it, not only for any kind of soil, but also without restriction for any mechanical states involved, stable or unstable, and over all ranges of instability, from deformation to failure, or liquefaction to subsequent reconsolidation in the case of sand. Similarly, the analysis performed can be static or dynamic, and provision can be made for any kind of external disruption affecting the ground. The analysis reported here concerns an event in which the ground resonates with the incoming seismic motion. The large shearing forces repeatedly acting on the soil elements are shown to induce loosening in the soil skeleton, which may result in local swelling and rising at the time of the earthquake. The analysis also shows that the input acceleration applied to the foundation (taken to mean the lower edge of the area analyzed) provokes vertical response movements at the surface, even when the acceleration wave consists only in a horizontal component. Further, it is found that the resultant acceleration wave has a very marked asymmetry in the vertical direction, whereas the waveform in the horizontal direction is symmetrical. This recalls the result of measurements obtained at the KiK-net seismograph station IWTH25 (West Ichinoseki) at the time of the 2008 Iwate-Miyagi earthquake, which indicated a similar powerful seismic motion with marked asymmetry in the vertical component only (Aoi et al., 2008³⁾). The peculiarities in the acceleration wave noted by these authors were a large upward pulse compared with a smaller downward one, the fact that downward acceleration appears to peak at around 1g, and the greater width of the waveform in its downward pulses than in its upward ones (Fig. 1). The given physical ground values, input seismic wave details, etc., required for the analysis are not based on the West Ichinoseki data, but nevertheless the distinctive nonlinear ground response measured there during the earthquake could also be confirmed in the results of the present analysis, using a continuum approximation to earth as an elastoplastic body (Fig. 2).

1) Asaoka, et al. (2002): An elasto-plastic description of two distinct volume change mechanisms of soils, *Soils and Foundations*, **42(5)**, 47-57.

2) Noda, et al. (2008): Soil-water coupled finite deformation analysis based on a rate-type equation of motion incorporating the SYS Cam-clay model, *Soils and Foundations*, **48(6)**, 771-790.

3) Aoi, et al. (2008): Trampoline effect in extreme ground motion, *Science*, **322**, 727-730.

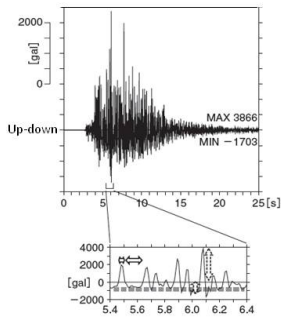


Fig. 1 Time history of ground surface acceleration response (observed results)³⁾

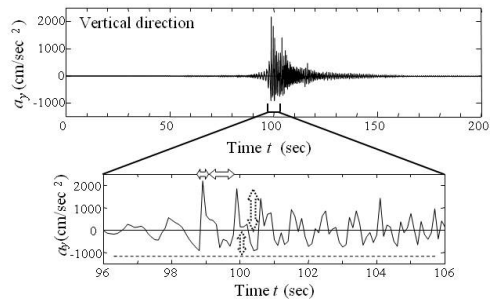


Fig. 2 Time history of ground surface acceleration response (analyzed results)

Keywords: strong motion earthquake, swelling/rising phenomenon, asymmetric waveform, elastoplastic constitutive equation, loosening, resonance

Japan Geoscience Union Meeting 2011

(May 22-27 2011 at Makuhari, Chiba, Japan)

©2011. Japan Geoscience Union. All Rights Reserved.



SSS023-17

Room:IC

Time:May 23 14:15-14:30

CMT inversion considering the isotropic component-Focal mechanism difference between a fault event and a volcanic one-

Takeshi Kurose^{1*}, Satoru Fujihara¹, Shinichi Akiyama¹, Hiroaki Yamanaka²

¹ITOCHU Techno-Solutions Corp., ²Tokyo Institute of Technology

In the CMT inversion of a fault-type event, it is commonly assumed that there is no contribution of the isotropic component. However, in the case of a volcanic event or an artificial one, it is considered that the isotropic component is not negligible. In this study, we develop a CMT inversion code considering the isotropic component, and investigate a focal mechanism difference between a fault-type event and a volcanic one by using the code.

Keywords: CMT inversion, isotropic component, fault-type earthquake, volcanic earthquake, focal mechanism, earthquake ground-motion characteristics

SSS023-18

Room:IC

Time:May 23 14:30-14:45

Near-real-time imaging of earthquake rupture by normalized short-period envelopes

Shigeki Aoki^{1*}, Yasuhiro Yoshida¹, Akio Katsumata¹

¹Meteorological Research Institute

1. Introduction

After a great earthquake, real-time estimations of rupture area and locations of asperities are important to assess hazards due to tsunami and ground shaking. However, it takes long time to analyze source process by the waveform inversion. Aoki et al. (2010, SSJ) developed a method for near-real-time imaging of earthquake rupture by normalized short-period envelopes, and succeeded in depicting rough image of rupture process of the 2003 Off Tokachi Eq. (TKEQ). In this study, we apply our method to the 1994 Far E off Sanriku Eq. (SREQ), and evaluate the accuracy for location and timing of the rupture.

2. Method

Our method is based on the Source-Scanning Algorithm [Kao & Shan, 2007]. It is applied for identifying the rupture plane. The brightness of a grid point is calculated by summing the amplitudes of normalized envelopes with the correction of the S-wave travel times at all stations. The grid points are arranged not on the prescribed fault plane, but in the 3D source volume. The composite image of the brightness of all grid points illuminates the locations and timings of seismic rupture (e.g. asperity). The normalized short-period (5-10Hz) envelopes give us an advantage of reducing the effect of site amplification factors, radiation patterns [Kamae et al., 1990] and surface waves [Izutani & Hirasawa, 1987]. In addition, our method is robust to outliers because the brightness is defined as the average amplitude of all stations, and is suitable for real-time processing.

3. Application to the SREQ

We used 17 JMA 87-type accelerometers within 500km from the epicenter. The grid points were arranged in and around the aftershock area (200km (NS) x 400km (EW) x 90km (depth)) at 2km interval. The brightness of each grid was calculated for 120 sec after the initial rupture.

The maximum of brightness (0.89) was appeared at 54s, and its location was 129km in N83W of the epicenter, and the depth was 26km. This point was close to the high frequency source [Sato et al. (1996), 51s, 137km in N82W, and 49km depth], except for the depth with low resolution. In the brightness snapshots from 27.5s to 63.0s, the peak brightnesses exceeded 0.7. The trace of the peak brightness almost corresponded to that of large slip area estimated by the waveform inversion [Nakayama & Takeo, 1997].

In this study, data length must be more than 5 minutes after the origin time, and it took about 15 minutes of calculation by an Intel Xeon X5550 (2.66GHz). For the TKEQ, the data length must be more than 3.5 minutes, and the computation time was about 4 minutes. To reduce the computation time, we plan to investigate the proper number of the grid points and to modify the code for parallel computing.

4. Discussion

The brightness image is interpreted as a superposition of a real rupture image and a blurring effect, which is due to a gap of station distribution, rupture duration and a wave scattering. In this section, we evaluate the blurring effect on the basis of the brightness images of point-source-like aftershocks and synthetic envelopes.

We estimated the M5.0 aftershock near the asperity of the TKEQ by the same station distribution as the main shock. The maximum was appeared at 1.0s, the location was 18km from the epicenter. In the case of the M5.6 aftershock of the SREQ, the peak was appeared at 5.0s, the location was 6km away. In both cases, the grid points having more than 0.7 in the brightness were distributed within 55km in horizontal distance, and ranged from -10s to 10s in time.

We compare the images calculated by the synthetic envelopes with and without scattering effect. The scattering effect is evaluated on the basis of the theory by Saito et al. (2002). Consequently, the image with scattering effect was more similar to that of the real aftershock. These results show that our method was influenced by scattering effect and the image was broadened.

Keywords: Near-real-time processing, Source process, The 1994 Far E Off Sanriku Earthquake

SSS023-19

Room:IC

Time:May 23 14:45-15:00

Uncertainty of Kinematic Source Inversion Solution by Resampling Test in Case of the 2007 Noto Hanto Earthquake

Kimiyuki Asano^{1*}, Tomotaka Iwata¹

¹DPRI, Kyoto University

Kinematic source inversion using strong motion and GPS data gives detailed image of the heterogeneous source rupture process during large earthquakes. The obtained source models have been used to discuss the relationship between the heterogeneous rupture process and the near-source strong ground motions and to develop the strong motion prediction technique based on the recipe (e.g., Iwata, 2009). However, there are critical discussion on the stability and reliability of the kinematic source inversion results, and an international project for source inversion validation was launched (e.g., Mai *et al.*, 2010). In this study, we analyze the stability and uncertainty of the kinematic source inversion solution by bootstrap approach using the data set for the 2007 Noto Hanto earthquake.

As for the 2007 Noto Hanto earthquake, we have already obtained the source rupture process by the multiple time-window linear waveform inversion method (Hartzell and Heaton, 1983) using the velocity waveform data at 12 strong motion stations of K-NET and KiK-net (0.05-1 Hz) and the horizontal static offset measured at 19 GPS stations of GEONET (Asano and Iwata, 2007). The one-dimensional velocity structure models for strong motion stations were optimized by the aftershock's waveform modeling. The relative weight between strong motion and GPS data and the smoothing strength were objectively determined by minimizing ABIC.

In this study, we generated 1000 data sets by randomly removing three strong motion stations and four GPS stations from the original data set. From 1000 solutions, we calculated the averages, standard deviations, and the coefficients of variation of the total seismic moment and the slip amount at each subfault. The average total seismic moment is 1.64×10^{19} Nm and average maximum slip is 4.8 m, those are comparable to the estimation by Asano and Iwata (2007). Those coefficients of variation are 9% and 11%, respectively. We will also investigate spatiotemporal characteristics of those statistical parameters in detail. From above analyses, we can conclude that we could obtain the reliable stable solution if we used efficient number of data and appropriate velocity structure model.

Acknowledgments: Strong motion data of K-NET and KiK-net of NIED and the daily coordinate data of GEONET of GSI are used in this study.

Keywords: kinematic source inversion, uncertainty, strong motion data, GPS data, the 2007 Noto Hanto earthquake

Japan Geoscience Union Meeting 2011

(May 22-27 2011 at Makuhari, Chiba, Japan)

©2011. Japan Geoscience Union. All Rights Reserved.



SSS023-20

Room:IC

Time:May 23 15:00-15:15

Influence of super-shear on simulated near-source ground motion from the 1999 Izmit earthquake

Hideo Aochi^{1*}, Virginie Durand², John Douglas¹

¹BRGM/RNSC, Orleans, France, ²ISTerre, Grenoble, France

We numerically simulate seismic wave propagation from the 1999 Mw7.4 Izmit, Turkey, earthquake, using a 3D finite difference method based on published finite source models obtained by waveform inversions. This earthquake has been reported, based on observations at the near-fault station SKR, as an example of super-shear rupture propagation towards the east. Although the modeled ground motion does show a characteristic Mach wave from the fault plane, it is difficult to identify any particular effects in terms of peak ground velocity, an important parameter in earthquake engineering. This is because the fault spatial heterogeneity is strong enough to mask the properties of super-shear rupture, which has been reported through several numerical simulations mostly based on homogeneous fault conditions. This study demonstrates the importance of studying ground motions for known earthquakes through numerical simulations based on finite-fault source models.

Keywords: ground motion, super-shear rupture, Izmit earthquake, finite source models, finite difference simulation

SSS023-21

Room:IC

Time:May 23 15:15-15:30

Strong motion simulation of the 2007/9/15 Peru earthquake; Effect of radiation pattern on atypical strong ground motions

Nelson Pulido^{1*}, Hernando Tavera², Zenon Aguilar³, Shoichi Nakai⁴, Fumio Yamazaki⁴

¹Nat. Res. Inst. Earth Sc. and Dis. Prev, ²Instituto Geofisico del Peru, ³Universidad Nacional de Ingenieria, ⁴Chiba University

The 2007 Mw8.0 Pisco earthquake was a thrust event originating at the interface of the Nazca and South-American plates, in a region slightly north of where the Nazca ridge encounters the trench and is being subducted beneath the Peru margin. The source area of the Pisco earthquake was located 160 km south-east of Lima, off-shore of the Pisco city, in a region filling the gap between the 1974, Mw8.0 Lima earthquake, and the 1996, Mw7.7 Nazca ridge earthquake. The source model of this earthquake displays two distinct asperities, the first one located near the hypocenter at a depth of 39 km, and the second one located 60 km to the South at a depth of 17km (Sladen et al., JGR, 2010). The source time function of this earthquake was also characterized by two episodes of moment release, the first one at 10s and the second and largest one at 80s, separated by a very low apparent rupture velocity of 1.5 km/s. These features suggest that the earthquake may have been characterized by a delayed rupture of two isolated events, each with a conventional rupture velocity. Ground motions from this earthquake are also characterized by two clear sub-events originating from each asperity, as can be observed from strong motion recordings of the mainshock at Lima (NNA), and Parcona (PCN) stations. The acceleration waveform at PCN station, which is located above the source area of the earthquake, is characterized by an atypical pattern, namely that the peak amplitude corresponding to the first sub-event is more than 5 times larger than the peak amplitude from the second sub-event, despite the fact that the second sub-event has a much larger moment release and is located closer to PCN. To explain this unusual pattern one may think of large differences in the propagation characteristics between asperities 1, 2 and PCN, or differences originating at the source. We may rule out the contribution of site-effects to explain this difference as we can assume it is the same for both sub-events.

Based on the aforementioned source model we simulated the strong ground motions at PCN and compare it with the observed record. Our simulations show that a variable radiation pattern across the fault plane can provide an appropriate explanation on the relative differences in amplitude for the two sub-events at PCN. The radiation pattern of S waves for a point source at the centroid of asperity 2 shows that the location of station PCN is coincident with a nodal plane of SH waves. Therefore the large seismic radiation released from this asperity is dramatically reduced at PCN by a very small radiation pattern coefficient. In contrast the seismic radiation from asperity 1 is modulated by a large radiation pattern coefficient, as its azimuth relative to PCN differs by approximately 45 degrees with respect to the asperity 2 to PCN azimuth, thus enhancing the source contribution to amplitudes from the first sub-event at PCN. On the other hand the source model of the Pisco earthquake displays a small average rise time for asperity 1 (around 1s), as compared to a large rise time for asperity 2 (around 7s), which may also have contributed to magnify the amplitudes from asperity 1.

Acknowledgements

This study is being conducted within the framework of a JICA/JST project entitled 'Enhancement of Earthquake and Tsunami Disaster Mitigation Technology in Peru'. The strong motion data at NNA and PCN stations belongs to the strong motion network of the Instituto Geofisico del Peru.

Keywords: 2007 Peru earthquake, Strong motion, radiation pattern, Nazca plate

SSS023-22

Room:IC

Time:May 23 15:30-15:45

Strong motion simulation for the 2004 Chuetsu earthquake with special reference to large velocity at Ojiya

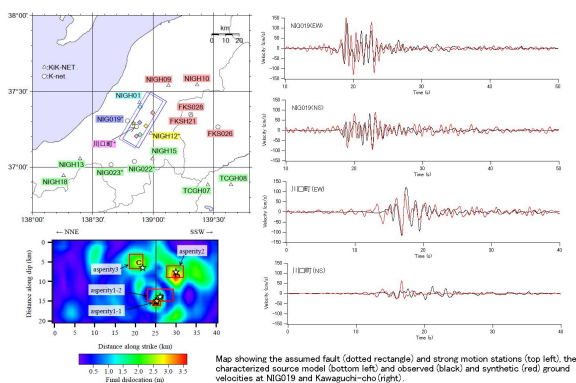
Atsushi Nozu^{1*}, Kimitoshi Sakai²

¹Port and Airport Research Institute, ²Railway Technical Research Institute

According to studies in the field of engineering seismology after the 1995 Hyogo-ken Nanbu earthquake, it was revealed that near-source velocity pulses can cause serious damage to structures (e.g., Kawase, 1998) and that these velocity pulses can be simulated using characterized source models quite accurately (e.g., Kamae and Irikura, 1998). These were the pulses that resulted from forward directivity effects. Since then, however, there have been many cases in which large amplitude (about 100 cm/s or more) ground velocities, which cannot be attributed to forward directivity effects, were observed in the near-source region of large crustal earthquakes in Japan. The strong ground motion observed at Ojiya during the 2004 Chuetsu earthquake is one of the examples. It is important from engineering point of view to investigate the validity of characterized source models for these cases.

For the 2004 Chuetsu earthquake, there have been several trials to construct characterized source models (e.g., Kamae et al., 2005) but none of them seemed to be quite successful in reproducing ground velocities including those at K-NET Ojiya and Kawaguchi-cho. In this study, the authors propose a new characterized source model, which is capable of reproducing near-source ground velocities including those at K-NET Ojiya and Kawaguchi-cho.

Empirical site amplification and phase characteristics were considered (Kowada *et al.*, 1998; Nozu *et al.*, 2009) in the simulation. There were two key factors that contributed to the reproduction of strong ground motions at K-NET ojiya in this study. One of them was selecting appropriate aftershock records to take into account phase characteristics. The other was taking into account nonlinear site response at K-NET Ojiya as revealed by Tokimatsu *et al.* (2006) and Tokimatsu and Sekiguchi (2006).



Keywords: strong ground motion, characterized source model, site amplification factor, phase, nonlinearity, The 2004 Chuetsu earthquake

SSS023-23

Room:IC

Time:May 23 15:45-16:00

Broadband Ground Motion Prediction for Miyagi-oki Earthquake Scenarios

Hiroe Miyake^{1*}, Kazuki Koketsu¹, Tetsu Masuda¹, Haruhiko Suzuki², Yasuhiro Kaida²

¹Earthq. Res. Inst., Univ. Tokyo, ²OYO Corp.

The omega-squared source model with a single corner frequency is widely used in the earthquake source analyses and ground motion simulations. Recent studies show that the Brune stress drop of subduction-zone earthquakes is almost half of that for crustal earthquakes for a given magnitude. On the other hand, the empirical attenuation relations and spectral analyses of seismic source and ground motions support the fact that subduction-zone earthquakes provide 1-2 times of the short-period source spectral level for crustal earthquakes. To link long- and short-period source characteristics is a crucial issue to perform broadband ground motion simulations. This discrepancy may lead the source modeling with double corner frequencies [e.g., Atkinson, 1993]. We modeled the lower corner frequency corresponding to the size of asperities generating for long-period (> 2-5 s) ground motions by the deterministic approach and the higher corner frequency corresponding to the size of strong motion generation area for short-period ground motions by the semi-empirical approach. We propose that the double corner source spectral model is expressed as a period-dependent source model consists of either the asperities in a long-period range or the strong motion generation area in a short-period range and the surrounding background area inside the total rupture area. The characterized source model has been the potential to reproduce fairly well the rupture directivity pulses seen in the observed ground motions. We explore the applicability of the double corner source spectral model to broadband ground motion simulations for the Mw 7.6 and Mw 7.3 Miyagi-oki earthquake scenarios along the Japan Trench. The Mw 7.6 scenario is similar to the source model of the 1978 Miyagi-oki earthquake. The double corner source spectral model, where the size and stress drop for strong motion generation areas are respectively half and double of those for asperities, worked well to reproduce broadband ground motion time histories and seismic intensity distribution of the 1978 Miyagi-oki earthquake.

This research was supported by the Integrated Research Project for Miyagi-oki Earthquakes from the Ministry of Education, Culture, Sports, Science and Technology (MEXT), Japan.

Keywords: broadband ground motion simulation, Miyagi-oki earthquake, characterized source model, Japan integrated velocity structure model, hybrid method

SSS023-24

Room:IC

Time:May 23 16:00-16:15

Study on New Recipe for Predicting Strong Ground Motions from Intra-slab Earthquakes

Toru Ishii^{1*}, Satoko Murotani², Sadayuki Kitagawa¹, Kojiro Irikura³

¹MEXT, Japan, ²ERI, Univ. of Tokyo, ³Aichi Institute of Technology

The Headquarters for Earthquake Research Promotion (HERP) have been making the long-term evaluation reports for inland crustal earthquakes along the major active faults and the major subduction-zone earthquakes which will occur in and around Japan in the future, and established the procedure to predict strong ground motions for scenario earthquakes, which has been named the Recipe. The objective of this study is to establish a new Recipe for intra-slab earthquakes.

Though both of inter-plate and intra-slab earthquakes belong to subduction-zone earthquakes, the present Recipe by HERP for subduction-zone earthquakes is fundamentally the one for inter-plate earthquakes. As for intra-slab earthquakes, few historical earthquakes have been observed, few data and knowledge have been obtained, and their characteristics have not been clarified enough. However in the last decade, some intra-slab earthquakes occurred, new knowledge was obtained from new data, and it is becoming necessary to consider the knowledge into the earthquake resistant design of important structures. Therefore, the Subcommittee for Evaluation of Strong Ground Motion of HERP has started studies to establish a new Recipe for intra-slab earthquakes.

Recently, procedures to make characteristic fault models of earthquakes were newly proposed, for example, Dan et al.(2006), Sasatani et al.(2006), Iwata and Asano(2010). Compared with inter-plate earthquakes, an intra-slab earthquake generates much more short-period seismic waves from its asperity with smaller size. Such characteristics of intra-slab earthquakes are important for the earthquake resistant design of short-period structures. Especially, Dan et al.(2006) and Sasatani et al.(2006) applied the empirical Green 's function method to the strong ground motion records from recent intra-slab earthquakes, and presented empirical relations between the combined area of asperities and the seismic moment, empirical relations between the short-period source spectra level and the seismic moment, respectively. In this study, a new Recipe for intra-slab earthquakes is proposed, focusing on the asperity area and the short-period source spectra level, which are evaluated by using the above mentioned empirical relations. Firstly, the asperity area and the short-period source spectra level are evaluated from the assumed seismic moment. Then the effective stress on the asperity and the average static stress-drop on the entire fault plane are evaluated theoretically. The inner and outer source parameters are calculated successively by using empirical and theoretical relations.

Keywords: subduction-zone earthquake, intra-slab earthquake, strong motion prediction, recipe, fault model, asperity